Quasi-classical trajectory investigation on the stereodynamics of Li + DF ($v = 1$–6, $j = 0$) → LiF + D reaction*

Zhang Ying-Ying(张莹莹)[a], Li Shu-Juan(李淑娟)[a], Shi Ying(石 英)[a]†, Xie Ting-Xian(解廷献)[b]‡, and Jin Ming-Xing(金明星)[a]

[a] *Institute of Atomic and Molecular Physics, Jilin University, Changchun* 130012, *China*
[b] *Department of Physics, Dalian Jiaotong University, Dalian* 116028, *China*

(Received 25 March 2014; revised manuscript received 3 July 2014; published online 10 October 2014)

In this paper, the stereodynamics of Li + DF → LiF + D reaction is investigated by the quasi-classical trajectory (QCT) method on the $^2A'$ potential energy surface (PES) at a relatively low collision energy of 8.76 kcal/mol. The scalar properties of the title reaction such as reaction probability and cross section are studied with vibrational quantum number of $v = 1$–6. The product angular distributions $P(\theta_r)$ and $P(\phi_r)$ are presented in the same vibrational level range. Moreover, two polarization-dependent generalized differential cross sections (PDDCSs), i.e., the $PDDCS_{00}$ and $PDDCS_{22+}$ are calculated as well. These stereodynamical results demonstrate sensitive behaviors to the vibrational quantum numbers.

Keywords: quasi-classical trajectory (QCT), stereodynamics, polarization-dependent generalized differential cross sections

PACS: 34.50.Lf, 82.20.Fd, 82.20.Kh **DOI:** 10.1088/1674-1056/23/12/123402

1. Introduction

Recently, plenty of investigations on the scalar and vector properties of chemical reactions have been carried out to explore the kinetics and stereodynamics.[1–7] As a benchmark in molecular reaction dynamics, the Li + HF → LiF + H reaction has been investigated both experimentally and theoretically.[8–14] In the area of experimentation, with the development of the crossed molecular beam techniques, Becker *et al*.[15] have measured an angular distribution of LiF product molecule, which is different from previous studies. In addition, the double differential cross sections have been worked out by Hobel *et al*.[16] and the results indicated that the scattering characteristics are strongly dependent on differential cross section. By using the transition state spectroscopy, the dynamics on the excited-state of Li + HF → LiF + H has been determined in a wavelength range of 570 nm–970 nm.[17] Meanwhile, many theoretical treatments have been presented in recent years. In 1997, a new fit to a more accurate MRDCI *ab initio* potential energy surface was constructed by Aguado and Paniagua,[18] and is used in our present work. Meanwhile, as a vital isotopic variant reaction of Li + HF → LiF + H, the title reaction Li + DF → LiF + D has gained considerable interest.[19–21] In 2009, Yuan and Zhao[19] investigated the collision energy influence on the Li + H(D)F → LiF + H(D) reaction, and the results showed that both the collision energy and the mass exert a significant effect on the stereodynamics of the two reactions. Later in 2011, using quasi-classical trajectory method, Cheng and Yue[20] investigated the kinetic properties of the initial vibrational and rotational conditions of Li + HF → LiF + H and its isotopic reactions at a collision energy of 110 meV.

In recent decades, experimental techniques[22–26] like crossed molecular beams[27–29] have paved the way for making the study of reaction stereodynamics feasible. In order to enrich our understanding of chemical reactions, such as vector correlations and product polarization, the quasi-classical trajectory (QCT) method has been developed[30–32] which presents a beneficial theoretical approach to the stereodynamical study on chemical reactions. Lately, it was developed and widely employed in calculating atomic and diatomic reactions.[33–36] Since their high accuracy in computing scalar properties, the quantum method (QM) and time-dependent wave packet method[37–39] have been extensively used in theoretical calculations. In contrast, the merits of the QCT method are less time consuming and convergent in a relatively low-energy area.

Thus far, we have studied the vibrational effect on Li + HF → LiF + H reaction[40] which has gained sensitive results. In order to explore the effect of its isotopic reaction, in our present work, we investigate the vibrational influences on the reaction probability, cross section and stereodynamical information of Li + DF → LiF + D reaction under the same conditions.

*Project supported by the Fund from the Jilin University, China (Grant No. 419080106440), the Chinese National Fusion Project for the International Thermonuclear Experimental Reactor (ITER) (Grant No. 2010GB104003), and the National Natural Science Foundation of China (Grant No. 10974069).

†Corresponding author. E-mail: shi_ying@jlu.edu.cn
‡Corresponding author. E-mail: xietingx@djtu.edu.cn

© 2014 Chinese Physical Society and IOP Publishing Ltd

2. Theory and computational methods

2.1. PES and the QCT calculations

The potential energy surface (PES) used in this work is the AP2-PES developed by Aguado and Paniagua.[18] It is worth mentioning that the existing PES has a potential well at the entrance channel and a nonlinear transition state was found to shift into its exit channel. The classical Hamilton's equations are numerically integrated in three dimensions. In this paper, the trajectories are initially set at an Li–DF internuclear separation of 10 Å. Under this circumstance, the collision energy is taken to be 8.76 kcal/mol with a batch of 2×10^4 trajectories running for each vibrational quantum number. The integration step size of 0.1 fs is used to ensure numerical stability and the convergence. The vibrational and rotational levels of the reactant molecule are chosen to be $v=1$–6, $j=0$, respectively. The accuracy of the numerical integration is verified by checking the conservations of the total energy and the total angular momentum for each trajectory.

2.2. Rotational alignment parameter and PDDCSs

The center-of-mass (CM) frame is employed in our calculations shown in Fig. 1. The z axis is parallel to the reagent initial relative velocity vector $\boldsymbol{k}$, and the y axis is perpendicular to the x–z scattering plane containing $\boldsymbol{k}$ and $\boldsymbol{k}'$. The θ_r is the angle between $\boldsymbol{j}'$ and $\boldsymbol{k}$, ϕ_r is the dihedral angle between the $\boldsymbol{k}$–$\boldsymbol{k}'$ and $\boldsymbol{k}$–$\boldsymbol{j}'$ which are referred to as the polar angle and the azimuth angle of the vector $\boldsymbol{j}'$, respectively, and θ_t is the scattering angle between $\boldsymbol{k}$ and $\boldsymbol{k}'$. All of these angles can be generated from the QCT dynamical calculations. The reaction probability and the cross section are defined as follows:

$$P_r=(N_r/N), \tag{1}$$

$$\sigma_r=\pi b_{\max}^2 P_r, \tag{2}$$

where N_r is the number of reaction trajectories and N is the total number of trajectories; the $b_{\max}$ is the maximum value of the impact parameter.

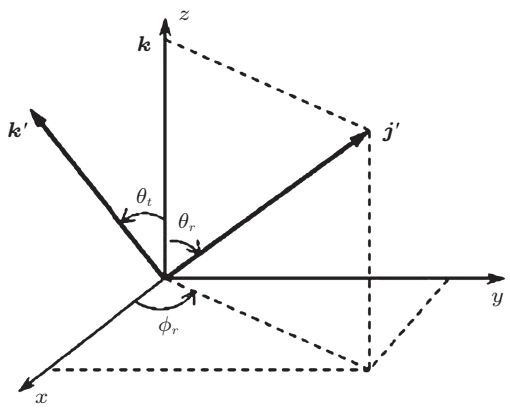


Fig. 1. Centre-of-mass coordinate system used to describe the $\boldsymbol{k}$, $\boldsymbol{k}'$, and $\boldsymbol{j}'$ correlations.

The functions $P(\theta_r)$, $P(\phi_r)$, and $P(\theta_r,\phi_r)$ are used in the following expansions, which are correspondingly defined in the following equations:[41–44]

$$P(\theta_r)=\frac{1}{2}\sum_k (2k+1)a_0^k P_k(\cos\theta_r), \tag{3}$$

with

$$a_0^2=\langle P_2(\cos\theta_r)\rangle=\langle P_2(j'\cdot k)\rangle=\frac{1}{2}\langle 3\cos^2\theta_r-1\rangle, \tag{4}$$

where the term $\langle P_2(j'\cdot k)\rangle$ is the average rotational alignment parameter which is also calculated in this work;

$$P(\phi_r)=\frac{1}{2\pi}\left(1+\sum_{n_{\text{even}}\geq 2} a_n\cos n\phi_r+\sum_{n_{\text{odd}}\geq 1} b_n\sin n\phi_r\right), \tag{5}$$

$$P(\omega_t,\omega_r)=\frac{1}{4\pi}\sum_{kq}[k]\,a_q^k C_{kq}(\theta_r,\phi_r)^*=\frac{1}{4\pi}\sum_k\sum_{q\geq 0}\left[a_{a\pm}^k\cos q\phi_r-a_{q\mp}^k\,\mathrm{i}\sin q\phi_r\right]C_{kq}(\theta_r,0), \tag{6}$$

where a_n, b_n, a_q^k, and C_{kq} can be seen in Refs. [45] and [46].

$$\frac{1}{\sigma}\frac{\mathrm{d}\sigma_{kq\pm}}{\mathrm{d}\omega_t}=\sum_{k1}\frac{[k_1]}{4\pi}S_{kq\pm}^{k1}C_{k1-q}(\theta_t,0), \tag{7}$$

$$\frac{1}{\sigma}\frac{\mathrm{d}\sigma_{k0}}{\mathrm{d}\omega_t}=0,\quad (k=\text{odd}), \tag{8}$$

$$\frac{1}{\sigma}\frac{\mathrm{d}\sigma_{kq+}}{\mathrm{d}\omega_t}=\frac{1}{\sigma}\frac{\mathrm{d}\sigma_{kq}}{\mathrm{d}\omega_t}+\frac{1}{\sigma}\frac{\mathrm{d}\sigma_{k-q}}{\mathrm{d}\omega_t}=0,\quad (k=\text{even},\ q=\text{odd or } k=\text{odd},\ q=\text{even}). \tag{9}$$

The $(1/\sigma)(\mathrm{d}\sigma_{kq\pm}/\mathrm{d}\omega_t)$ is the polarization-dependent generalized differential cross sections (PDDCSs). In our present work, two PDDCSs, i.e., the $(2\pi/\sigma)(\mathrm{d}\sigma_{00}/\mathrm{d}\omega t)$ and $(2\pi/\sigma)(\mathrm{d}\sigma_{22+}/\mathrm{d}\omega t)$ are calculated.

3. Results and discussion

The QCT method used in our work offers a quicker way of performing the stereodynamical calculation especially on more than one heavy atom included in the reactant molecules. In our present work, all the stereodynamical sections are depicted in three dimensions. The reaction probability P_r and the average rotational alignment parameter $\langle P_2(j'\cdot k)\rangle$ are plotted together as shown in Fig. 2. It is obvious that with increasing the vibrational quantum number, the distribution of the reaction probability P_r shows a first increasing and then decreasing trend and the peak is at $v=4$. Additionally, the values of $\langle P_2(j'\cdot k)\rangle$ are all negative and become smaller, which demonstrates a weaker trend of the product alignment. We can also obtain that the $\langle P_2(j'\cdot k)\rangle$ is a linear function of the vibrational excitation, indicating that the product rotational angular momentum vector $\boldsymbol{j}'$ tends to be anisotropic with respect to $\boldsymbol{k}$.

Figure 3 illustrates the total reaction cross section as a function of the vibrational level, which is calculated from Eq. (2). Thus, we obtain the maxima of impact parameter $b_{\max}$ corresponding to different vibrational levels, and they are listed in Table 1. As shown in Fig. 3, with the successive increment of vibrational level from $v = 1$ to 6, the reaction cross section increases rapidly, which implies a strong energy barrier on the PES and the vibrational levels have a positive effect on the scalar properties of the title reaction.

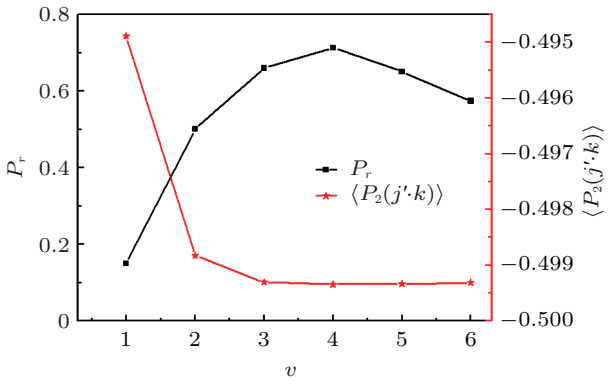


Fig. 2. (color online) Reaction probability P_r and the average rotational alignment parameter $\langle P_2(j'\cdot k)\rangle$ versus vibrational level from $v = 1$ to $v = 6$.

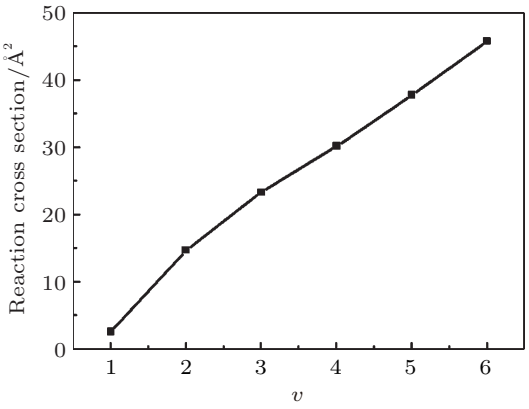


Fig. 3. Variation of reaction cross section for the title reaction with vibrational level v in a range of 1–6.

Table 1. Maxima of the impact parameter $b_{\max}$ for $v = 1$–6.

Vibrational level	1	2	3	4	5	6
$b_{\max}$	2.3532	3.0603	3.3532	3.6745	4.3021	5.0401

The product angular distributions of $P(\theta_r)$ representing the $\boldsymbol{k}$–$\boldsymbol{j}'$ correlation at vibrational levels $v = 1$–6 are displayed in Fig. 4. As can be seen in the figure, for different vibrational quantum numbers, the peaks of $P(\theta_r)$ are all at $\theta_r = 90^\circ$ and symmetric with respect to 90° which implies that the product rotational angular momentum vector $\boldsymbol{j}'$ is perpendicular to the direction of the reagent relative velocity $\boldsymbol{k}$. Besides, the peaks of $P(\theta_r)$ become higher and narrower as the vibrational quantum number increases, indicating that the product alignment becomes stronger at a high vibrational excitation state.

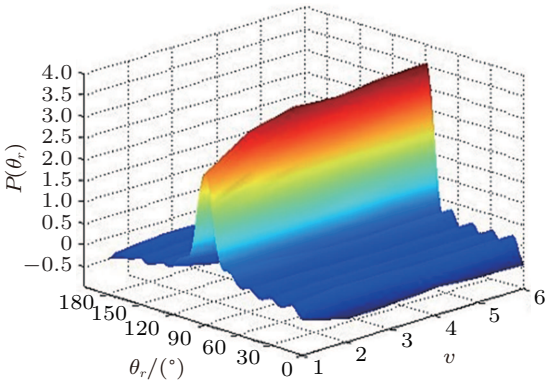


Fig. 4. (color online) Distributions of $P(\theta_r)$ reflecting $\boldsymbol{k}$–$\boldsymbol{j}'$ correlations at different vibrational levels $v = 1$ to 6 for the reagent rotational excitation.

Figure 5 displays the dihedral angle distributions of $P(\phi_r)$ which describe the $\boldsymbol{k}$–$\boldsymbol{k}'$–$\boldsymbol{j}'$ correlation. In this paper, without prejudice to the overall results, we only show the $P(\phi_r)$ distributions of $v = 2$, $v = 4$, and $v = 6$ with the order from inside to outside. It can be seen that the $P(\phi_r)$ tends to be antisymmetric with respect to $\phi_r = 180^\circ$, directly reflecting the strong polarization of the angular momentum of the Li + DF → LiF + D reaction that is induced by the AP2-PES. Peaks at all calculated vibrational levels are equally situated at $\phi_r = 90^\circ$ and $\phi_r = 270^\circ$, which reflects that the product rotational angular momentum vector $\boldsymbol{j}'$ is not only aligned but also oriented. Meanwhile, we can also see that as the vibrational level increases, the peak at $\phi_r = 90^\circ$ becomes higher and narrower while it becomes lower and broader when $\phi_r = 270^\circ$ and the peak at $\phi_r = 90^\circ$ is much higher than that at $\phi_r = 270^\circ$, which reflects that the product rotational angular momentum vector $\boldsymbol{j}'$ prefers to orient along the positive direction of y axis. The antisymmetry of $P(\phi_r)$ can be described qualitatively by the impulse model given by Wang *et al.*[41] Based on these studies, the antisymmetry of $P(\phi_r)$ most likely results from the repulsive energy between D–F molecules, which leads to the violation of the symmetry when the reaction occurs. The product angular momentum vector $\boldsymbol{j}'$ is defined as $\boldsymbol{j}' = \boldsymbol{L}\sin^2\beta + \boldsymbol{J}\cos^2\beta + \boldsymbol{J}_1 m_{\rm A}/m_{\rm B}$ and $\boldsymbol{J}_1 = (\mu_{\rm BC}R)^{1/2}(r_{\rm AB} \times r_{\rm CB})$, where $\boldsymbol{L}$ is the reagent orbital angular momentum, the term $\boldsymbol{L}\sin^2\beta + \boldsymbol{J}\cos^2\beta$ is symmetric, whereas $\mu_{\rm BC}$ is the reduced mass of the BC molecule; R is the repulsive energy; $r_{\rm AB}$ and $r_{\rm CB}$ are the unit vectors, where atom B points to atoms A and C, respectively. In the Li + DF → LiF + D reaction, the term $\boldsymbol{J}_1 m_{\rm A}/m_{\rm B}$ shows a preferential direction for the effect of repulsive energy, causing the right-handed product rotation in planes to be parallel to the scattering plane.

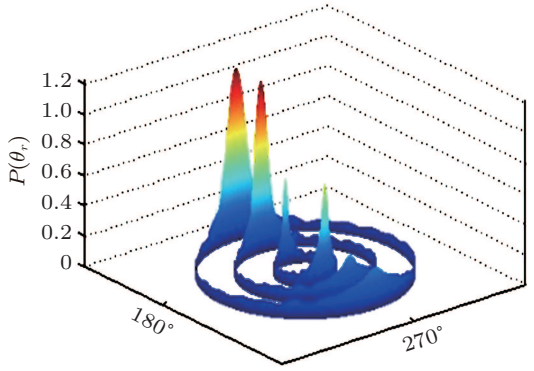


Fig. 5. (color online) Distributions of $P(\phi_r)$ with respect to the $\boldsymbol{k}$–$\boldsymbol{k}'$ plane depicted from inside to outside: $v = 2$, $v = 4$, and $v = 6$, respectively.

In order to further verify the above-mentioned points, we also plot the angular momentum polarization in the form of $P(\theta_r, \phi_r)$ averaged over all scattering angles as shown in Fig. 6. In order to save the space and stay consistent with Fig. 5, we take the vibrational states at $v = 2$, 4, 6 with only the joint $P(\theta_r, \phi_r)$ distributions. Obviously, the distributions of $P(\theta_r, \phi_r)$ are in good accordance with the distributions of $P(\theta_r)$ and $P(\phi_r)$.

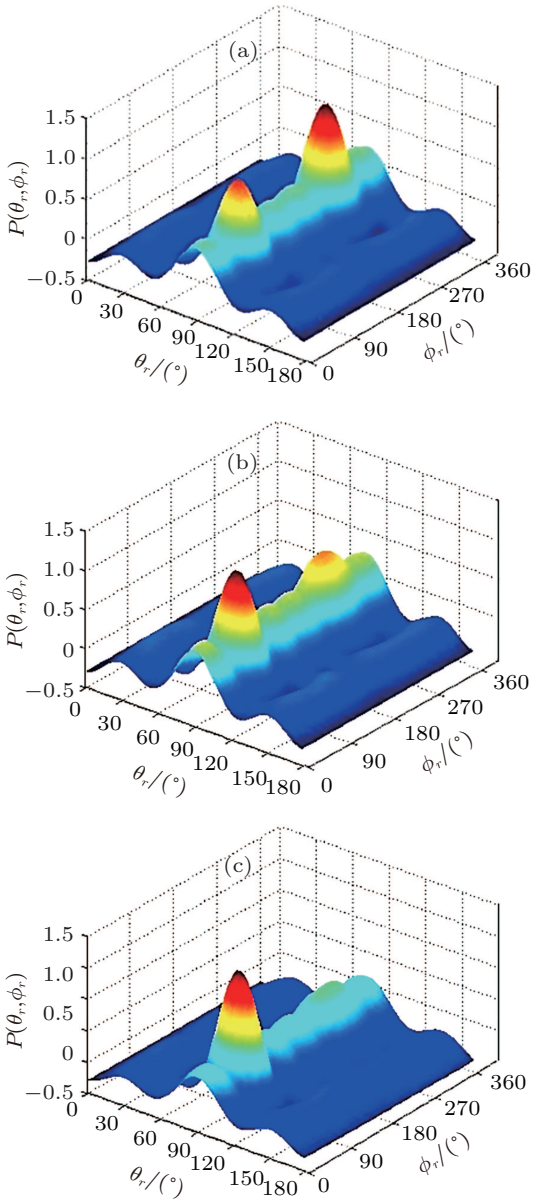


Fig. 6. (color online) Distributions of $P(\theta_r, \phi_r)$ with peaks and valleys at different vibrational levels: (a) $v = 2$; (b) $v = 4$; (c) $v = 6$.

The PDDCSs which describe the $\boldsymbol{k}$–$\boldsymbol{k}'$–$\boldsymbol{j}'$ correlation and the scattering direction of the LiF product for the title reaction are plotted in Fig. 7. In our paper, we only discuss $(2\pi/\sigma)(\mathrm{d}\sigma_{00}/\mathrm{d}\omega t)$ and $(2\pi/\sigma)(\mathrm{d}\sigma_{22+}/\mathrm{d}\omega t)$. The PDDCS_{00} has a simple different cross section (DCS) only describing the $\boldsymbol{k}$–$\boldsymbol{k}'$ correlation or the scattering direction of LiF product which has no relation with the orientation and alignment of $\boldsymbol{j}'$. In Fig. 7(a), with the increase of the states, the forward scattering of the product LiF becomes stronger while the backward scattering turns weaker and tends to the sideward scattering. One of the PDDCSs with $q \neq 0$, the PDDCS_{22+} which provide information about the dihedral angle ϕ_r, is shown in Fig. 7. As can be seen in Fig. 7(b), at the extremities of the forward and backward scattering, the values of PDDCS_{22+} are zero at all vibrational levels, whereas the values are nonzero when away from both ends of the forward and backward scattering. Meanwhile, for $v = 1$ to $v = 6$, all of the values are negative, which indicates a significant alignment of the product in the direction of y axis. Moreover, an obvious peak is seen in the vicinity of $\theta_t = 150^\circ$ which implies a strong polarization of the product rotational angular momentum vector $\boldsymbol{j}'$.

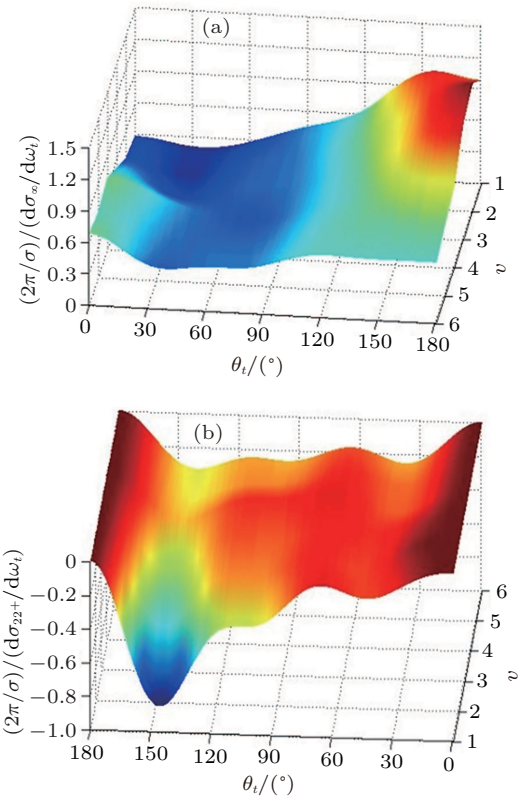


Fig. 7. (color online) Two polarization-dependent generalized differential cross sections of the vibrational levels ranging from $v = 1$ to $v = 6$: (a) $(2\pi/\sigma)(\mathrm{d}\sigma_{00}/\mathrm{d}\omega)$; (b) $(2\pi/\sigma)(\mathrm{d}\sigma_{22+}/\mathrm{d}\omega)$.

4. Conclusions

By applying the QCT method to the AP2-PES, we investigate the vibrational effect on the title reaction at a relatively low collision energy of 8.76 kcal/mol. With the increase of the vibrational level, the probability indicates a first increasing and then decreasing behavior. The phenomenon of $\langle P_2(j' \cdot k)\rangle$ demonstrates a weak product alignment. Due to the energy barrier height on the PES and the increase of $b_{\max}$, the cross section reveals an increasing trend. Moreover, a series of stereodynamical information is also presented. The distribution of $P(\theta_r)$ representing the $\boldsymbol{k}$–$\boldsymbol{j}'$ correlation indicates a strong rotational alignment of the product. The distribution of $P(\phi_r)$ reflects that the product rotational angular momentum vector $\boldsymbol{j}'$ is not only aligned but also oriented along the positive direction of y axis. The stereodynamical results of the above two distributions are further proved by the distribution of $P(\theta_r, \phi_r)$. The PDDCS_{00} implies that as vibrational level increases, the forward scattering becomes stronger, meanwhile, the backward scattering turns weaker and then tends to the sideward scattering. The PDDCS_{22+} presents a strong polarization of the product rotational angular momentum vector $\boldsymbol{j}'$. In summary, comparison between the results of Li + HF $\rightarrow$ LiF + H reaction reveals a greater vibrational effect on both scalar properties and stereodynamics of the Li + DF $\rightarrow$ LiF + D reaction.

Acknowledgment

Many thanks to Prof. Han Ke-Li for providing the stereodynamics program, and also to the High Performance Computing Center of Jilin University, China for providing the computation facilities.

References

[1] Loesch H J and Stienkemeier F 1993 *J. Chem. Phys.* **99** 9598
[2] Han K L, He G Z and Lou N Q 1996 *J. Chem. Phys.* **105** 8699
[3] Aoiz F J, Brouard M and Enriquez P A 1996 *J. Chem. Phys.* **105** 4964
[4] Miranda M P D, Clary D C, Castillo J F and Manolopoulos D E 1998 *J. Chem. Phys.* **108** 3142
[5] Jorfi M, Honvault P, Halvick P, Lin S Y and Guo H 2008 *Chem. Phys. Lett.* **462** 53
[6] Liu Y F, Gao Y L, Zhai H S, Shi D H and Sun J F 2009 *Int. J. Mol. Sci.* **10** 2146
[7] Lu R F, Wang Y H and Deng K M 2013 *J. Comput. Chem.* **34** 1735
[8] Pruett J G and Zare R N 1976 *J. Chem. Phys.* **64** 1774
[9] Karny Z and Zare R N 1978 *J. Chem. Phys.* **68** 3360
[10] Parker G A, Laganá A, Crocchianti S and Pack R T 1995 *J. Chem. Phys.* **102** 1238
[11] Aoiz F J, Martínez M T, Menéndez M, Sáez-Rábanos V and Verdasco E 1999 *Chem. Phys. Lett.* **299** 25
[12] Aoiz F J, Martínez M T, Menéndez M and Sáez-Rábanos V 2001 *J. Chem. Phys.* **114** 8880
[13] Lara M, Aguado A, Paniagua M and Roncero O 2000 *J. Chem. Phys.* **113** 1781
[14] Weck P F and Balakrishnan N 2005 *J. Chem. Phys.* **122** 154309
[15] Becker C H, Casavecchia P, Tiedemann P W, Valentini J J and Lee Y T 1980 *J. Chem. Phys.* **73** 2833
[16] Hobel O, Bobbenkamp R, Paladini A, Russo A and Loesch H J 2004 *Phys. Chem. Chem. Phys.* **6** 2198
[17] Hudson A J, Oh H B, Polanyi J C and Piecuch P 2000 *J. Chem. Phys.* **113** 9897
[18] Aguado A and Paniagua M 1997 *J. Chem. Phys.* **106** 1013
[19] Yuan M H and Zhao G J 2009 *J. Mol. Struc. Theochem.* **916** 23
[20] Cheng J and Yue X F 2011 *Chin. Phys. Lett.* **28** 083102
[21] Tan R S, Liu X G and Hu M 2012 *Chin. Phys. Lett.* **29** 123101
[22] Loesch H J, Stenzel S and Wüstenbecker B 1991 *J. Chem. Phys.* **95** 3841
[23] Han K L, Zhang L, Xu D L, He G Z and Lou N Q 2001 *J. Phys. Chem. A* **105** 2956
[24] Cohen E A, McRae G A, Tan T L, Friedl R R, Johns J W C and Noel M 1995 *J. Mol. Spectrosc.* **173** 55
[25] Cronkhite J M and Wine P H 1998 *Int. J. Chem. Kinet.* **30** 555
[26] Brouard M, Lambert H M, Rayner S P and Simons J P 1996 *Mol. Phys.* **89** 403
[27] Balucani N, Beneventi L, Casavecchia P, Volpi G G, Kruss E J and Sloan J J 1994 *Can. J. Chem.* **72** 888
[28] Hobel O, Paladini A, Russo A, Bobbenkamp R and Loesch H J 2004 *Phys. Chem. Chem. Phys.* **6** 2198
[29] Parson J M and Lee Y T 1972 *J. Chem. Phys.* **56** 4658
[30] Becker C H, Casavecchia P, Tiedemann P W, Valentini J J and Lee Y T 1980 *J. Chem. Phys.* **73** 2833
[31] Neumark D M, Wodtke A M, Robinson G N, Hayden C C and Lee Y T 1985 *J. Chem. Phys.* **82** 3067
[32] Bradforth S E, Arnold D W, Neumark D M and Manolopoulos D E 1993 *J. Chem. Phys.* **99** 6345
[33] Wang M L, Han K L and He G Z 1998 *J. Phys. Chem. A* **102** 10204
[34] Cai M Q, Zhang L, Tang B Y, Chen M D, Yang G W and Han K L 2000 *Chem. Phys.* **255** 283
[35] Zhang W Q, Li Y Z, Xu X S and Chen M D 2010 *Chem. Phys.* **367** 115
[36] Chen M D, Han K L and Lou N Q 2003 *J. Chem. Phys.* **118** 4463
[37] Chen M D, Tang B Y, Han K L, Lou N Q and Zhang J Z H 2003 *J. Chem. Phys.* **118** 4463
[38] Xie T X, Zhang Y, Zhao M Y and Han K L 2003 *Phys. Chem. Chem. Phys.* **5** 2034
[39] Chu T S, Zhang Y and Han K L 2006 *Int. Rev. Phys. Chem.* **25** 201
[40] Li S J, Shi Y, Xie T X and Jin M X 2012 *Chin. Phys. B* **21** 013401
[41] Wang M L, Han K L and He G Z 1998 *J. Chem. Phys.* **109** 5446
[42] Zhang Y Y, Shi Y, Xie T X, Jin M X and Hu Z 2013 *Chin. Phys. B* **22** 083402
[43] Xu W W, Liu X G, Luan S X, Sun S S and Zhang Q G 2009 *Chin. Phys. B* **18** 339
[44] Liu S L and Shi Y 2010 *Chin. Phys. Lett.* **27** 123103
[45] Zhang J, Chu T S, Dong S L, Yuan S P, Fu A P and Duan Y B 2011 *Chin. Phys. Lett.* **28** 093403
[46] Yao C X and Zhao G J 2013 *Can. J. Chem.* **91** 387